Journal of Magnetics 4(4), 131-135 (1999)

Study on the HDDR Characteristics of the Nd-Fe(-Co)-B(-Ga-Zr)-type Alloys

S. W. Shon, H. W. Kwon, D. I. Kang, Yoon. B. Kim[1] and W. Y. Jeung[1]

Pukyong National University, Pusan, Korea
[1]Korea Institute of Science and Technology, Seoul, Korea

(Received 30 August 1999)

The HDDR characteristics of the Nd-Fe-B-type isotropic and anisotropic HDDR alloys were investigated using three types of alloys: alloy A ($Nd_{12.6}Fe_{81.4}B_6$), alloy B ($Nd_{12.6}Fe_{81.3}B_6Zr_{0.1}$), and alloy C ($Nd_{12.6}Fe_{68.8}Co_{11.5}B_6Ga_{1.0}Zr_{0.1}$). The alloy A is featured with the isotropic HDDR character, while alloy B and C are featured with the anisotropic HDDR character. Hydrogenation and disproportionation characteristics of the alloys were examined using DTA under hydrogen gas. Recombination characteristics of the alloys were examined by observing the coercivity variation as a function of recombination time. The present study revealed that the alloy C exhibits slightly higher hydrogenation and disproportionation temperatures compared to the alloy A and B. Recombination of the anisotropic alloy B and C takes place more rapidly with respect to the isotropic alloy A. The intrinsic coercivities of the recombined materials rapidly increased with increasing the recombination time and then showed a peak, after which the coercivities decreased gradually. The degraded coercivity was, however, recovered significantly on prolonged recombination treatment. Compared with the isotropic HDDR alloy A the anisotropic HDDR alloy B and C are notable for their greater recovery of coercivity. The significant recovery of coercivity was accounted for in terms of the development of well-defined smooth grain boundary between the recombined grains on prolonged recombination.

1. Introduction

The HDDR (hydrogenation, desorption, disproportionation, recombination) process [1, 2] is well known to be an effective production way of a high coercivity Nd-Fe-B-type alloy powder directly from the ingot material. Employing the HDDR process to the Nd-Fe-B ternary alloy leads usually to an isotropic powder. Interestingly, it has been known that an anisotropic powder can also be prepared using the HDDR process if the ternary Nd-Fe-B standard alloy is modified by additive elements such as Co, Ga, Zr, Hf [3-5]. The principal purpose of the present study is the comparison of the HDDR characteristics of the Nd-Fe-B-type isotropic and anisotropic HDDR alloys. The magnetic properties of the HDDR-treated Nd-Fe-B-type materials are influenced decisively by the condition of each step during the HDDR treatment. Among the various HDDR steps the recombination is one of the most important step determining the magnetic properties (in particular coercivity) of the HDDR-treated materials. In this article, therefore, a particular emphasis was placed on the recombination characteristics of the alloys

2. Experimentals

Three types of Nd-Fe-B-type alloys were used in the present study, and their compositions are tabulated in Table 1. The alloys were prepared by an induction melting. The prepared alloys were homogenised at 1000 °C for 3 days (alloy A, B) or 6 days (alloy C). The ternary alloy A is generally known to show an isotropic HDDR character. On the other hand, the alloy B and C containing Co, Ga, and/or Zr are known to exhibit an anisotropic HDDR character. The composition of alloy C is included in the composition range of a commercially available anisotropic Nd-Fe-B-type HDDR powder. The hydrogenation and disproportionation characteristics were examined using a DTA under hydrogen gas (1.8 kgf/cm^2). Desorption and recombination characteristics of the alloys were examined using the coercivity variation as a function of desorption and recombination time. Microstructural development during the HDDR was examined by means of TEM using solid-HDDR [6, 7] treated samples. X-ray powder diffraction with Cu-K_α radiation was utilised to analyse the phase change during the HDDR treatment.

Table 1. Chemical composition of the alloys

alloy	Nd	Fe	Co	B	Ga	Zr	HDDR nature
A	12.6	81.4		6			isotropic
B	12.6	81.3		6		0.1	anisotropic
C	12.6	68.8	11.5	6.	1.0	0.1	anisotropic

Magnetic characterisation was performed by means of a VSM. For the VSM measurement the powder sample was wax-bonded and then magnetised with a pulsing magnetic field of 45 kOe.

3. Results And Discussion

DTA results representing the hydrogenation and disproportionation characteristics of the alloys are shown in Fig. 1. As can be seen, two exothermic peaks appear on heating the alloys under hydrogen gas up to around 800 °C. The thermal event at lower temperature may be due mainly to the hydrogenation of the $Ne_2Fe_{14}B$ matrix phase in alloy, and the event at higher temperature to the disproportionation of the hydrided matrix phase. It appears that the alloy C exhibits slightly higher hydrogenation and disproportionation temperatures compared to the alloy A and B. It is notable that the heat flow (area covered by the thermal peak) for hydrogenation of alloy C is much smaller compared to that of the alloy A or B. This indicates that the alloy C up-takes hydrogen significantly smaller amount compared to other alloys. The amount of hydrogen absorbed on the disproportionation seems to be more or less same for the alloys investigated.

In order to examine correctly the recombination character of the alloys a prerequisite that the materials are under fully hydrogenated and disproportionated state should be fulfilled. The alloys, therefore, were hydrogenated during heating (7 °C/min) under hydrogen gas up to 800 °C and then disproportionated by holding it at the temperature for 2 hrs. Phase analyses of the disproportionated materials were performed by means of XRD, and the obtained representative diffraction spectrum (for the alloy B) is shown in Fig. 2. The diffraction patterns for the disproportionated alloy A and C were observed to be almost identical with that of the alloy B. As can be seen from the diffraction spectrum the disproportionated material consists mainly of Nd-hydride and α-Fe which are products of disproportionation of the $Nd_2Fe_{14}BH_x$. This indicates that the materials have been fully disproportionated. Full disproportionation of the material under the condition mentioned above was again confirmed by observing the microstructure by means of TEM. For the preparation of the TEM sample the alloy B was hydrogenated and disproportionated in a solid-HDDR manner. The previous result in the present author's lab revealed that the kinetics of disproportionation of a Nd-Fe-B-type alloy in solid-HDDR manner was much more sluggish than in the conventional manner [7]. Therefore, the material was disproportionated for longer period of 3 hrs in solid-HDDR manner. This disproportinated material (crushed powder) was then subjected to an XRD, and the obtained spectrum was found to be identical with that shown in Fig. 2. The same material in solid form was subjected to a TEM observation, and the result is shown in Fig. 3. It can be seen that the disproportionated materials composed of a very fine mixture of mainly Nd-hydride and α-Fe, in which the hydride phase is surrounded by the α-Fe, indicating that whole sample has been fully disproportionated. This particular microstructure consisting of Nd-hydride rod surrounded by a α-Fe was also reported by other group [8].

The materials fully disproportinated were subjected to a recombination under vacuum at 800 °C. The variation of the intrinsic coercivity of the materials was monitored as a function of recombination time, and the results are shown in Fig. 4. It appears that the intrinsic coercivities of all the alloys rapidly increase with increasing the recombination time in early stage of the recombination and then show a peak. After showing a peak the coercivities decrease gradually. Coercivities of the anisotropic alloy B and C reach peak value more rapidly compared to that of the isotropic alloy A. This indicates that the recombination of anisotropic alloy B and C takes place more rapidly with respect to the isotropic alloy A. Also included in the Fig. 4 is the variation of the intrinsic coercivity of the sample (alloy B) treated in a solid-HDDR manner [9]. This coercivity variation for the

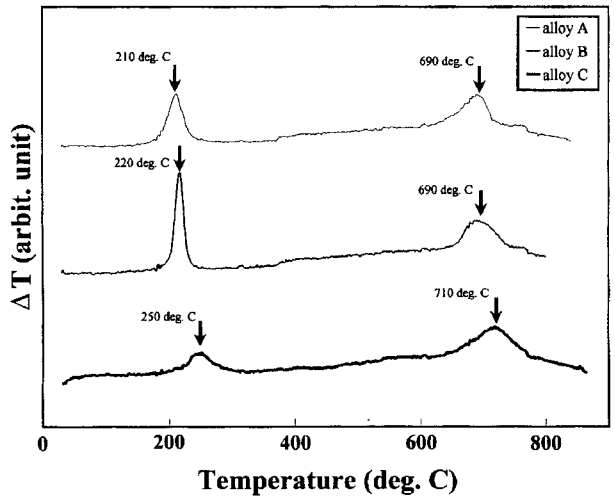

Fig. 1. DTA traces for the alloy A, B and C under H_2 gas.

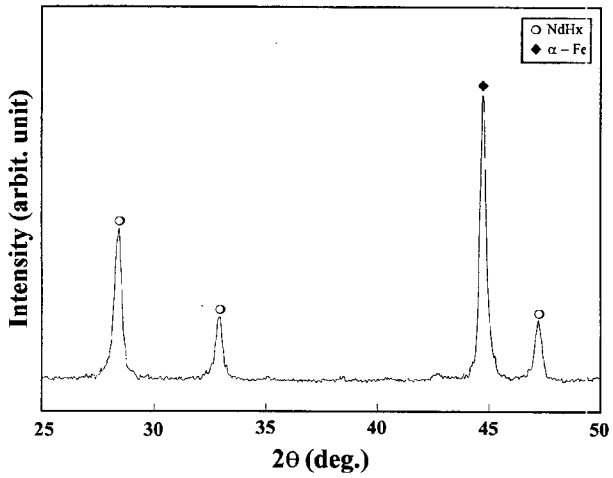

Fig. 2. X-ray diffraction spectrum of the fully disproportionated alloy B.

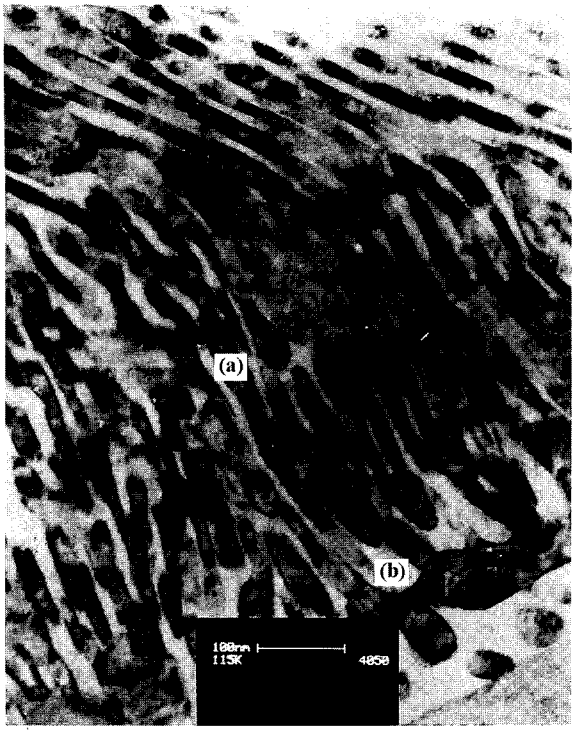

Fig. 3. TEM micrograph showing the microstructure of the alloy B fully disproportionated in solid manner: (a) NdH_x (b) α-Fe.

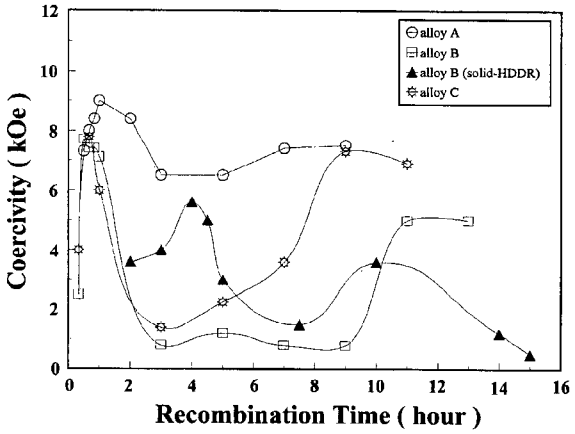

Fig. 4. Variations of the intrinsic coercivity of HDDR-treated alloys as a function of recombination time.

solid HDDR-treated material was examined in order to find out a condition for the preparation of TEM sample. The material HDDR-treated in a conventional manner usually comes out in powder form, thus not suitable for TEM observation. It is, therefore, desirable to use a material in solid form even after the HDDR treatment. As is the case for the conventional HDDR materials, the solid HDDR-treated material also shows a similar coercivity variation with exception that the general kinetics is much slower and the peak coercivity is significantly lower than those of the materials treated in conventional manner. Phase analysis and microstructural examination of the optimally recombined material showing the peak coercivity were performed by means of XRD and TEM using a solid HDDR-treated

Table 2. Coercivity variation during the recombination treatment

alloy	A	B	C
(a) initial peak coercivity (kOe)	9.0	7.7	7.8
(b) degraded coercivity (kOe)	6.5	1.0	1.5
(c) recovered coercivity (kOe)	7.5	5.0	7.3
degradation ((b)/(a))	0.72	0.13	0.19
recovery ((c)/(b))	1.15	5.00	4.87

sample (alloy B). The obtained X-ray diffraction spectrum showed that the disproportionated phases were fully recombined into $Nd_2Fe_{14}B$ phase. The observed microstructure is shown in Fig. 5. It can be seen that the initial coarse $Nd_2Fe_{14}B$ grain (initial grain size: 10~30 μm) has been restructured into a very fine grains ranging from 0.1 to 0.5 μm. This grain size range was obtained by measuring the size of the smallest and the largest grain in several areas in the sample. This fine grain size comparable to the critical single domain size (~0.3 μm) of the $Nd_2Fe_{14}B$ compound may be responsible for the high intrinsic coercivity of the optimally recombined material.

Interestingly, however, we observed that the degraded coercivity due to the over-recombination was recovered significantly on prolonged recombination as shown in Fig. 4. The possible excessive evaporation of the Nd from the alloy on prolonged treatment under vacuum was suppressed by changing the atmosphere to under Ar gas (pressure: 1 kgf/cm^2) after showing a peak coercivity. It appears that the

Fig. 5. TEM micrograph showing the microstructure of the optimally recombined material (solid HDDR-treated alloy B).

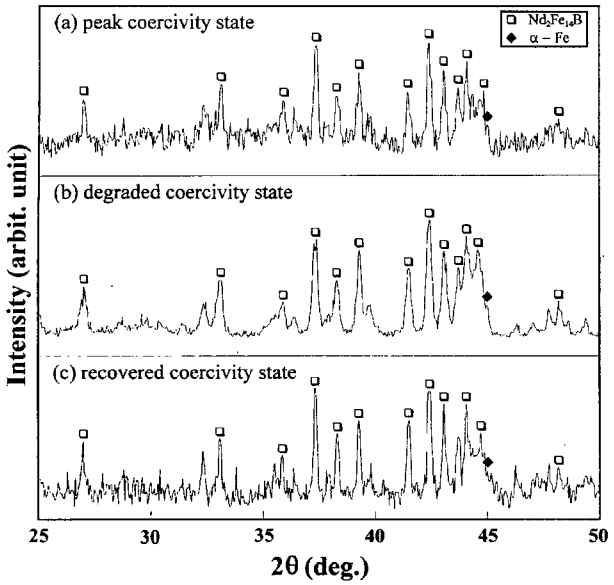

Fig. 6. X-ray diffraction spectrum for the alloy B HDDR-treated in solid manner with different recombination times at 800 °C : (a) 0.5 (b) 7 (c) 10 hours.

coercivity recovery is more profound in the anisotropic HDDR alloy B and alloy C with respect to the ternary isotropic HDDR alloy A as tabulated in Table 1. In order to understand the coercivity recovery observed on the prolonged recombination the microstructural examination and phase analysis of the materials under different conditions were performed by means of TEM and XRD. These examinations were undertaken using a solid HDDR-treated sample (alloy B). The microstructures of the samples corresponding to the degraded coercivity (recombined for 7 hrs) and to the recovered coercivity (recombined for 10 hrs) were examined. It is found that the microstructures of both samples are similar with each other except for a slightly greater grain size in the materials (0.3~2.0 μm) corresponding to the degraded coercivity state compared to the material (0.5~2.0 μm) corresponding to the recovered coercivity state. XRD phase analyses of the samples corresponding to the peak, degraded or recovered coercivity state also showed almost identical results as shown in Fig. 6. However, a close examination of the microstructure showed some difference between the two samples particularly at the grain boundary between the recombined grains (Fig. 7). There seems to be a well-defined smooth grain boundary in the material with recovered coercivity, which is different from a poorly defined grain boundary in the material with degraded coercivity. The underlying cause of the coercivity recovery on prolonged recombination is not understood precisely at the moment, but in our opinion, the most likely explanation for the recovery of coercivity is the development of a well-defined smooth grain boundary between the recombined grains. The poorly defined grain boundary in the material corresponding to the degraded coercivity may act as an easy nucleation site for a reversed domain under applied demagnetising field, thus resulting in a poor coercivity. On the

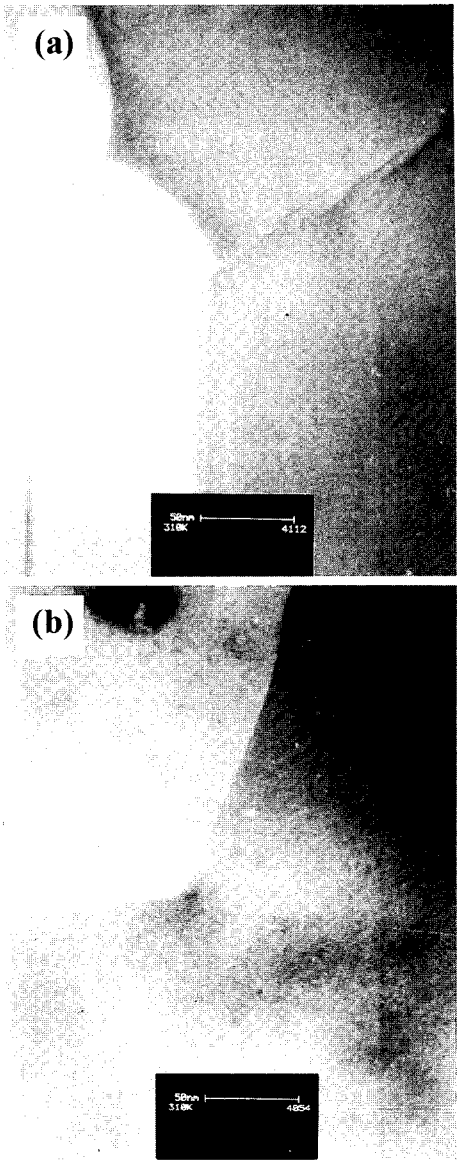

Fig. 7. Close examinations of the grain boundary regions of the prolong-recombined materials corresponding to (a) degraded and (b) recovered coercivity states (solid HDDR-treated alloy B).

contrary, the well-defined smooth grain boundary in the material at recovered coercivity may hardly act as a nucleation site for the reversed domain, resulting in an appreciable coercivity.

4. Conclusions

The HDDR characteristics of the Nd-Fe-B-type isotropic and anisotropic HDDR alloys were investigated. It has been found that the alloy C exhibits slightly higher hydrogenation and disproportionation temperatures compared to the alloy A and B. Recombination of the anisotropic alloy B and C takes place more rapidly with respect to the isotropic alloy A. The intrinsic coercivities of the recombined materials rapidly increased with increasing the recombination time and then showed a peak, after which the coercivities

decreased gradually. The degraded coercivity was, however, recovered significantly on prolonged recombination treatment. Compared with the isotropic HDDR alloy A the anisotropic HDDR alloy B and C are notable for their greater recovery of coercivity. The significant recovery of coercivity was accounted for in terms of the development of well-defined smooth grain boundary between the recombined grains on prolonged recombination.

Acknowledgement

The authors would like to gratefully acknowledge that part of the present work was supported by the Korea-UK Science and Technology Collaboration Fund under contract No. IU-01-001.

References

[1] I. R. Harris, Proc. 12th Intl. Workshop on Rare-Earth Magnets and Their Applications, Canberra, Australia, 347 (1992).

[2] T. Takeshita and R. Nakayama, Proc. 12th Intl. Workshop on Rare-Earth Magnets and Their Applications, Canberra, Australia, 670 (1992).

[3] R. Nakayama, T. Takeshita, M. Itakura, N. Kuwano and K. Oki, J. Appl. Phys., **76**(1), 412 (1994).

[4] H. Nakamura, S. Sugimoto, T. Tanaka, M. Okada, and M. Homma, J. Alloys and Compounds, **222**, 136 (1995).

[5] H. W. Kwon, IEEE Transactions on Magnetics, **32**, 4398 (1996).

[6] X. J. Zhang, P. J. McGuiness and I. R. Harris, J. Appl. Phys., **69**, 5838 (1991).

[7] H. W. Kwon and S. J. Kang, J. Appl. Phys., **83**, 7130 (1998).

[8] O. Gutfleisch, N. Matzinger, J. Fidler and I. R. Harris, J. Magn. Magn. Mat., **147**, 320 (1995).

[9] S. W. Shon and H. W. Kwon, Journal of Magnetics, **4**(2), 46 (1999).